Torres-Carrasco, M. & Puertas, F. (2017). Waste glass as a precursor in alkaline activation: Chemical process and hydration products. *Construction and Building Materials, 139*, 342–354.

DOI: 10.1016/j.conbuildmat.2017.02.071

Waste glass as a precursor in alkaline activation: chemical process and hydration products

M. Torres-Carrasco[1*] and F. Puertas[1]

[1]Eduardo Torroja Institute for Construction Sciences (IETcc-CSIC)

*Corresponding author: e-mail: mtorres@ietcc.csic.es

Abstract

This paper discusses the results of alkali-activating waste glass in pursuit of a new type of alkali activated materials (AAMs). Waste glass pastes were prepared with different alkaline activators (NaOH, NaOH/Na_2CO_3, sodium silicate hydrate and KOH) with different concentrations and cured for 20 h at 85°C and at 99 % or 6.5 % relative humidity to assess the effect of these variables on paste mechanical strength and microstructure. Compressive strength performance was better at the higher alkaline concentrations and when the pastes were cured at low relative humidity (6.5 %), which induced low porosity (MIP) and high specific surface (BET). Irrespective of the type of activator or curing process, the main reaction product was a Si-high, Al-low gel. As a raw material for alkaline cement manufacture, waste glass delivered compact, high- strength cementitious skeletons.

Keywords: waste glass; alkali-activated materials; mechanical behaviour; microstructure; curing conditions

1 Introduction

The alkaline activation of aluminosilicates is a well-known alternative to portland cement [1–4]. Aluminosilicates may be of natural (primarily clay) origin [5–8] or derived from industrial by-products, such as glassy blast furnace slag [8–12] or fly ash [13–15]. When these precursors are dissolved in alkaline solutions they condense and polymerise, generating so-called alkali-activated materials (AAMs) or geopolymers, depending on the chemical composition of the starting material used (rich or poor in CaO or Al_2O_3) and the final composition of the main reaction product. These materials, a new type of inorganic polymers with cementitious properties, are regarded as good candidates for applications including refractory panels [15] and the encapsulation of radioactive materials [16].

The possible use of other aluminosilicate materials as a solution to possible metakaolin or fly ash shortages is an area of particular interest. If their suitability for alkaline activation is confirmed, studies might then be conducted on their use as compositional correctors or supplements for more conventional geopolymers. Glass might be one such type of precursor [17]. Compositionally speaking, glass is comparable to its crystalline source materials with one exception: due to the cooling to which the molten material is subjected, it has a disorderly structure which might, a priori, be compatible with use in alkaline cement production.

The amount of urban and industrial waste has increased the world over in the last few decades [17]. Glass is an inert material under common environmental conditions that can be recycled in many ways without altering its chemical properties. Waste glass collection and management are, then, increasingly common elements of environmental policy in the developed world. According to EU data, Europeans recycle over eight million tonnes of glass containers yearly. In Spain over 700 000 tonnes of glass, or 59 glass containers per capita, were deposited in specific street-side bins and recycled in 2015 [18], for a recycle rate of approximately 70 %. Waste glass must meet a series of requirements for reuse in the manufacture of other glass articles, however. The tendency is to collect and sort urban and industrial waste glass by type. Even so, the mix of glass types, chemical compositions and particle sizes involved renders its reuse by conventional technological processes highly complex. As a result, from 10 to 30 % of waste glass is not recyclable for these purposes and alternative valorisation pathways must be sought.

One possible outlet for such waste is the construction industry. Many studies were conducted In the nineteen sixties on the possibility of using crushed waste glass as concrete aggregate [19–21]. Over the last 10 years, due to the high costs of eliminating waste glass and in the wake of European and US legislation on the environmental impact of the use of natural aggregate, such research has been renewed [22–28].

Papers [29–31] have also been published on the use of waste glass as a raw material to produce cement, given that its main chemical component is SiO_2. One of the concerns addressed in those papers is how glass alkalis might affect cement clinker minerals and how much alkali might remain in the clinker or affect the walls of the kiln. Both depend on the amount of waste glass used as a raw material: small replacement ratios can yield good results [30].

Recent studies [30,32] have explored the pozzolanic properties of waste glass and its use as a cement replacement in concrete manufacture. A number of benefits would ensue from the

reuse of waste glass in cement and concrete production: environmental conservation, longer landfill life, significant energy savings and lower greenhouse gas emissions.

The feasibility of using vitreous urban and industrial waste as a source of silica to wholly or partially replace sodium silicate (waterglass) in the alkaline activation of slag and fly ash has likewise been researched [33–38]. The process entails the partial dissolution of the waste glass in highly alkaline media ($NaOH/Na_2CO_3$ and NaOH) to obtain the type of silicon-rich solution that has been shown to be usable as an alternative to commercial sodium silicate activators. These waste glass-based alternative solutions are less energy-intensive and more eco-friendly than waterglass, which is economically and environmentally problematic to manufacture, for it calls for heating SiO_2 and Na_2CO_3 to temperatures of over 1000°C. For every kilogramme of sodium silicate produced, an estimated 1.5 kg of CO_2 is emitted into the atmosphere [39].

Synthesised glasses has been used as a precursor in geopolymer preparation [40–43]. The CaO content in synthesised glass and the Si/Al ratios of the starting material are variables that must be borne in mind for their possible effect on the mechanical properties and microstructure of the gels forming during alkaline activation [40]. The initial proportions of oxides used to generate the vitreous phase must be carefully controlled to ensure that the chemical composition of the aluminosilicate precursor optimises alkaline activation and the production of high performance cements [40].

Very few studies [44–47] have been conducted on the alkaline activation of urban and industrial waste glass, however, i.e., on the suitability of such waste as a prime material (or precursor) for activation. This study aimed to determine how intrinsic variables such as the nature and concentration of the alkaline activator and curing conditions affect glass activation and the microstructure of the reaction products. That involved assessing the mechanical strength and microstructure of the mixes prepared with alkali-activated waste glass.

2 Experimental procedures

2.1 Materials

Soda-lime-silica glass sourced from an industrial and urban waste management plant at Ajalvir, Madrid, Spain, was used in this study (**Figure 1**). Waste glass used was a mix of of different colours glass, crushed and ultimately ground to a particle size of < 45 μm and specific surface area of 1.75 cm^2/g [33–35].

The chemical composition given in **Table 1** confirms that it consisted primarily in SiO_2, Na_2O and CaO.

Figure 1. Treatment of waste glass of different colours (from a recycle plant at Ajalvir, Madrid, Spain) to obtain a particle size of < 45 µm for subsequent alkaline activation: **A)** clear waste glass; **B)** green waste glass; **C)** brown waste glass; **D)** mixed waste glass (used in the study)

Table 1. Chemical composition of waste glass (wt%) (XRF)

% wt	CaO	SiO_2	Al_2O_3	MgO	Fe_2O_3	Na_2O	K_2O	LoI*
Waste glass	11.75	70.71	2.05	1.17	0.52	11.71	1.08	0.83

*LoI: loss on ignition

The waste glass was activated with different solutions (**Table 2**). Panreac analytical grade (98 % pure) NaOH and (99.8 %) Na_2CO_3 were used; Merck analytical grade (99 % pure) KOH was used; and a Merck commercial waterglass (27 wt% SiO_2; 8 wt% Na_2O; 65 wt% H_2O) solution

with a SiO_2/Na_2O ratio of 0.86 was used. Moreover, two alternative solutions to commercial waterglass were used:

- a $NaOH/Na_2CO_3$ solution with the preceding components plus 25 g of dissolved glass as an alternative to commercial waterglass [33,35]. This is a solution resulting from 6 hours at 85°C of chemical treatment to obtain an alternative to commercial sodium silicate.
- a likewise NaOH solution with the preceding component plus (15 g per mL) waste glass as an alternative to commercial waterglass [34].

In both cases, to prepare the alternatives solutions to a commercial sodium silicate, the procedure was as follows: the waste glass with a particle size < 45 µm is brought into contact with the alkaline solution ($NaOH/Na_2CO_3$ or NaOH) during a stirring time of 6 hours and a temperature of 85˚C. After this time, the solution was filtered to be used as an alternative solution in the activation of the waste glass.

Table 2. Paste preparation: activation conditions

Sample name	Activator type	L/S	pH	% Na_2O	SiO_2/Na_2O	Curing process	
						Temperature (°C)	Humidity (%)
N/C	$NaOH/Na_2CO_3$	0.4	13.37	5.0	-	85	99.0
N/C	$NaOH/Na_2CO_3$	0.4				85	6.5
N/C+25g	*$NaOH/Na_2CO_3$-glass	0.4	13.40	5.0	0.86	85	99.0
N/C+25g	*$NaOH/Na_2CO_3$-glass	0.4				85	6.5
WG 0.86	Waterglass	0.4	13.80	5.0	0.86	85	99.0
WG 0.86	Waterglass	0.4				85	6.5
N10	NaOH	0.4	14.10	9.75	-	85	99.0
N10	NaOH	0.4				85	6.5
N10+15g	**NaOH-glass	0.4	13.60	9.75	0.11	85	99.0
N10+15g	**NaOH-glass	0.4				85	6.5
N10+15Wg	NaOH-waterglass	0.4	13.80	8.41	0.19	85	99.0
N10+15Wg	NaOH-waterglass	0.4				85	6.5
KOH	***KOH-10M	0.4	14.94	-	-	85	99.0
KOH	***KOH-10M	0.4				85	6.5

- * Solution prepared by dissolving 25 g of waste glass in 100 mL of $NaOH/Na_2CO_3$ [33]
- ** Solution prepared by dissolving 15 g of waste glass in 100 mL of 10 M NaOH [34]
- *** 10M KOH solution

2.2 Sample preparation and test methods

Paste specimens measuring 1x1x6 cm were prepared from the waste glass and aforementioned activators at a liquid/solid ratio of 0.4. The conditions for activating and preparing the waste glass are given in **Table 2**.

Two curing methods were used.

- Method 1: sealed mould curing [48]. Used in prior research, this procedure ensures that humidity is held constant to prevent quick setting [49–51] and carbonation [52] while the material sets and hardens. The trial consisted of placing the moulds with the fresh paste in water-containing sealed individual plastic bags to prevent evaporation during initial oven curing for 20 hours at 85 °C and 99 % relative humidity. RH was logged continuously with an EL-USB-2-LCD temperature (-35 °C-80°C) and relative humidity (0 %-100 %) sensor.
- Method 2: the pastes were placed in sealed individual plastic bags with no water. The specimens were cured at 85 °C for 20 hours, during which the relative humidity, held at approximately 6.5 %, was monitored constantly with the EL-USB-2-LCD data logger described above.

The prismatic specimens were tested for compressive strength after 24 hours of curing. After the strength tests, the pastes were frozen in acetone/ethanol to detain the hydration/activation reactions prior to Hg intrusion porosimetry (MIP), BET, XRD, FTIR, SEM and BSEM/EDX exploration on the following instruments.

- Mechanical strength tests were conducted to failure on an Ibertest Autotest 200/10 hydraulic press as specified in European standard EN 196-1 at a rate of 2 400 N/s ± 200 N/s. Compressive strengths was determined on 1 day specimens.
- Total porosity and pore size distribution were found with Hg intrusion porosimetry (MIP) on a Micromeretics Autopore IV 9500 analyser able to exert pressure of up to 32 000 Psi (equivalent to pore sizes down to 0.0067 µm).
- BET specific surface area measurements, pore size distribution and nanoporosity were found from nitrogen adsorption isotherms generated by a Micromeritics ASAP 2010 analyser.
- The XRD patterns for the samples were recorded on a Bruker AXS D8 Advance diffractometer fitted with a Lynxeye super speed XR detector and a 2.2-kW Cu anode. No monochromator was used. The scanning range, from (2θ) 5° to 50°, was covered in

a 24 hour period. The instrument was set at 40 kW and 30 mA and the sample was not rotated during scanning.

- The FTIR spectra were obtained from 64 scans of compressed KBr pellets containing 1.0 mg of sample in 300 mg of KBr run on an ATIMATTSON Genesis Series FTIR-TM spectrometer operating in a range of 4000 to 400 cm^{-1}.
- Carbon-coated samples were examined under a JOEL JSM 5400 scanning electron microscope fitted with a solid-state backscattered electron detector (SEM) and a LINK-ISIS energy dispersive (BSEM/EDX) analyser.

3 Results

3.1 Mechanical strength and porosity (MIP and BET)

The 1-day compressive strength values are depicted in **Figure 2A**. The activated waste glass exhibited strength ranging from 17 MPa to 88 MPa, depending on the activator and curing conditions. The highest performance was observed in the specimens cured at 6.5 % relative humidity, for which the values were 50 % to 75 % greater than in the specimens cured at high humidity for nearly all the activators (**Figure 2B**). The exception was the specimens activated with a 10 M KOH solution, in which no strength differences were observed between the two curing conditions.

The nature of the activator played a significant role in paste strength development. Of the solutions studied, the lowest performance was delivered by $NaOH/Na_2CO_3$ (pH = 13.3), with values on the order of 29 MPa (**Figure 2A**), which declined to 17.1 MPa when 25 g of waste glass was added to that solution as an alternative to commercial sodium silicate, yielding a pH of 13.4.

A possible explanation for such low mechanical strength may lie in the pH values (around 13.4) (**Table 2**). As pH governs aluminosilicate dissolution, which favours nucleation or condensation and polymerisation, it plays a crucial role in activating these materials. Nonetheless, when a commercial sodium silicate (waterglass) with a SiO_2/Na_2O modulus of 0.86 and pH of 13.8 was used, the strength measured was on the order of 54 MPa. As the liquid/solid ratio (L/S = 0.4) was identical in all the systems, however, when the commercial sodium silicate solution was used, the paste had a lower consistency which may have partially explained the higher mechanical strength observed [53]. Moreover, the reactivity of Si from a commercial sodium silicate is better than the dissolve silicon from waste glass.

When the glass pastes were activated with a high OH^- concentration (such as characteristically used to activate fly ash), mechanical strength rose. The best results were observed for the NaOH-glass waste solution (N10+15g), which delivered strength of 88 MPa. Torres-Carrasco and Puertas [34] observed the same strength performance in fly ash activated with this alternative to commercial sodium silicate, prepared by dissolving the waste glass in the presence of heat [35].

Lastly, with the 10 M KOH solution as an activator, the waste glass attained strength of around 50 MPa, a value lower than found for the Na^+ ion-containing media. As the K^+ cation dissolves less of the Ca and Mg present in the starting material, less reaction product precipitates [54,55].

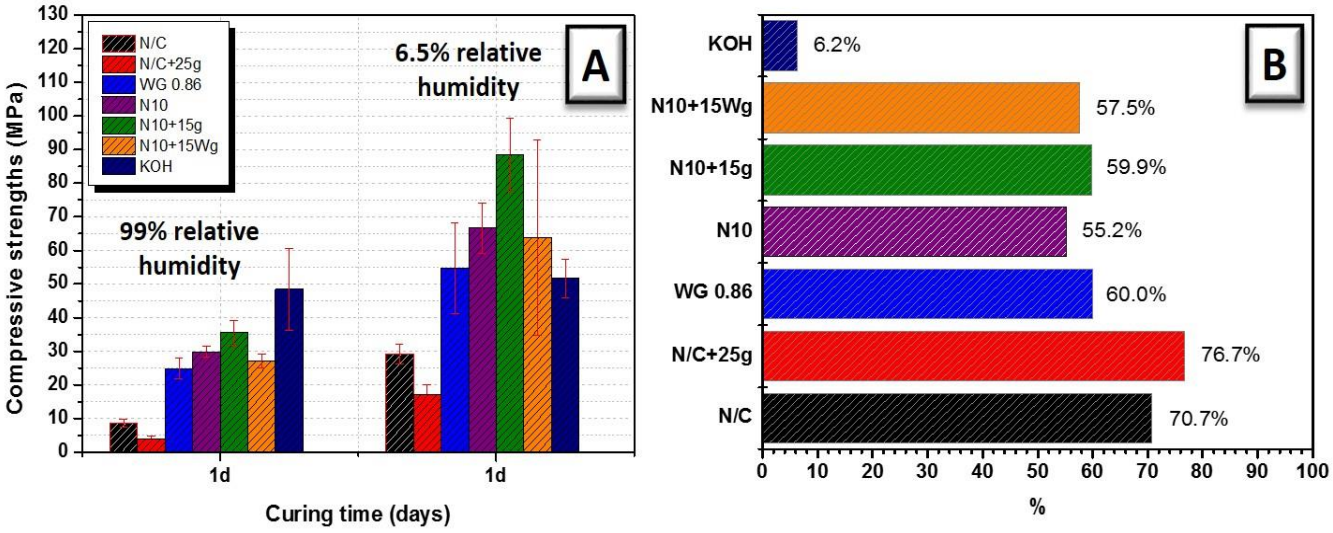

Figure 2. A) Compressive strength for waste glass activated with different activating solutions and cured at high (99 %) or low (6.5 %) relative humidity; **B)** percentage difference between high RH (99%) and low RH (6.5%) curing conditions

3.1.1 Hg intrusion porosimetry

Total porosity was determined in the systems exhibiting the best mechanical strength, i.e., the specimens cured at low (6.5 %) relative humidity. The total porosity and pore size distribution (in the 100 µm to 0.1 µm range) for the pastes are shown in **Figure 3**, where the porosity values are given in percentage of the total sample volume. The waste glass pastes activated

with the NaOH/Na_2CO_3-glass exhibited the highest total porosity (29.72 %). The presence of silicon from the glass waste did not favour 1-day mechanical strength development. In contrast, the commercial sodium silicate (waterglass) reduced porosity, thereby raising mechanical strength.

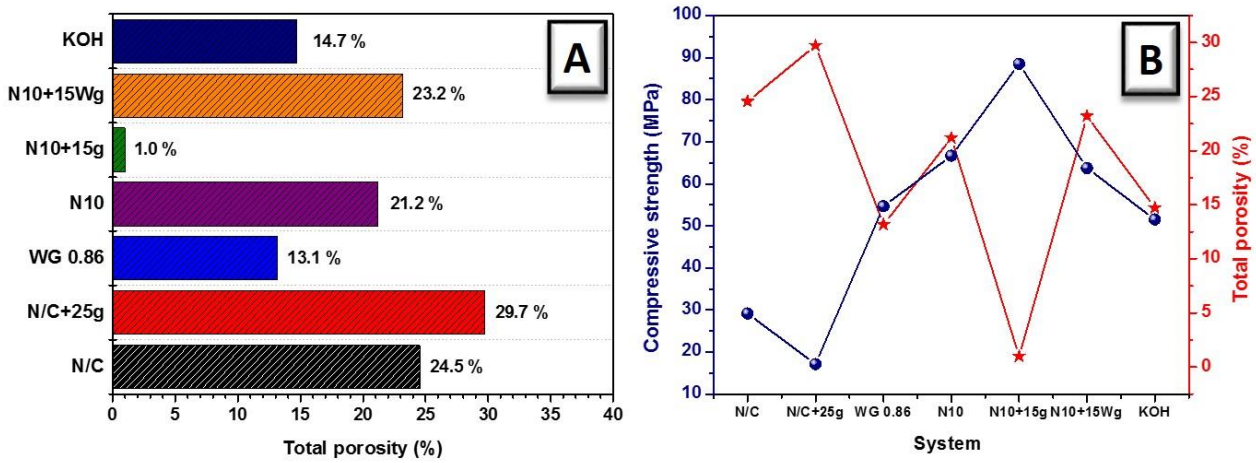

Figure 3. Glass waste pastes activated with different solutions and cured at 6.5 % relative humidity: **A)** pore size distribution vs total porosity; **B)** compressive strength vs total porosity

The waste glass pastes activated with NaOH-glass (N10+15g) showed the lowest total porosity, at around 1 %. That finding was consistent with the strength values of up to 88 MPa obtained for this system (**Figure 3B)**.

3.1.2 BET and nanoporosity

The differences in mechanical strength found in waste glass pastes activated with different activators may also be explained by the specific surface of the samples, and indirectly by the microporosity of the reaction products. The specific surface was observed to vary between the samples with the highest and lowest compressive strength (N10+15g and N/C+25g, respectively). In low (6.5 %) relative humidity curing, the sample activated with the NaOH-glass solution had a specific surface 12 % higher than the pastes hydrated with NaOH/Na_2CO_3-glass and 26 % higher than those activated with KOH (**Figure 4A**). **Figures 4 B), C)** and **D)** show that pores under 1 nm, associated with gel formation, were present in the three aforementioned systems.

Figure 4A shows how curing in different RH conditions affected the specific surface and pore size of the pastes activated with a given solution. At 6.5 % relative humidity the specific surface of samples N10+15g was 21 % higher than in the respective sample cured at 99 % relative humidity, whilst in the N/C+25g material the difference was 11 %. In contrast, the waste glass pastes activated with 10 M KOH exhibited very similar specific surface and pore size values (**Figure 4D**) irrespective of the relative humidity at which they were cured, which was consistent with the similar mechanical strength found for the respective specimens. Here also, the smaller ionic radius of Na^+ than K^+ would explain the lesser mobility of the potassium ion and hence less intense waste glass dissolution.

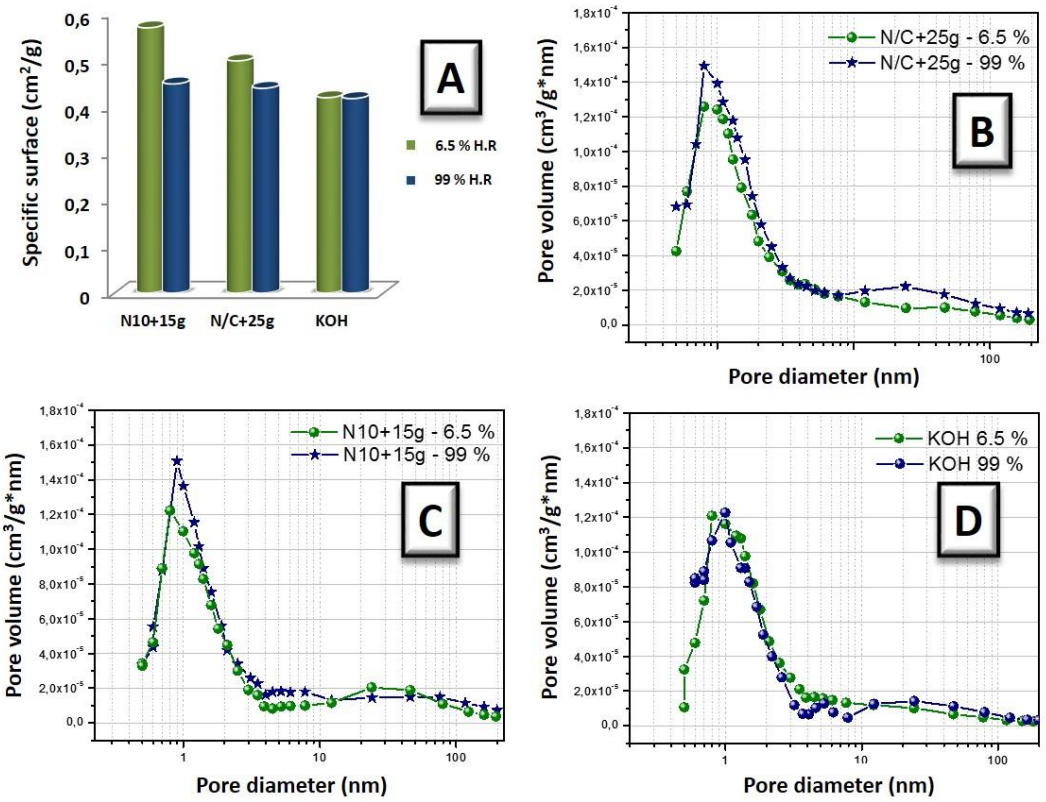

Figure 4. Waste glass paste cured at 6.5 % or 99 % relative humidity: specific surface for **A)** N10+15g, N/C+25g and KOH; pore size distribution for **B)** N10+15g, **C)** N/C+25g and **D)** KOH

3.2 Characterisation of reaction products

In light of the strength and porosity findings that revealed that the best results were obtained with low relative humidity curing, the main reaction products in the pastes prepared under those conditions were characterised mineralogically and microstructurally.

- XRD and FTIR

The 1 day diffractograms for the waste glass and the pastes prepared with the activators studied are reproduced in **Figure 5**. The unhydrated soda-lime waste glass was amorphous with low range structural order. The respective XRD trace exhibited no reflections attributable to any identifiable crystallised compound, but only an amorphous hump (**Figure 5**).

The XRD findings showed that the reaction products in the pastes hydrated with each activator retained an amorphous structure with scantly any crystalline phases. The amorphous hump was shifted slightly toward higher (30°-32°) 2-theta values, however, a finding attributed to a higher Na_2O content in the main reaction products formed [44,56].

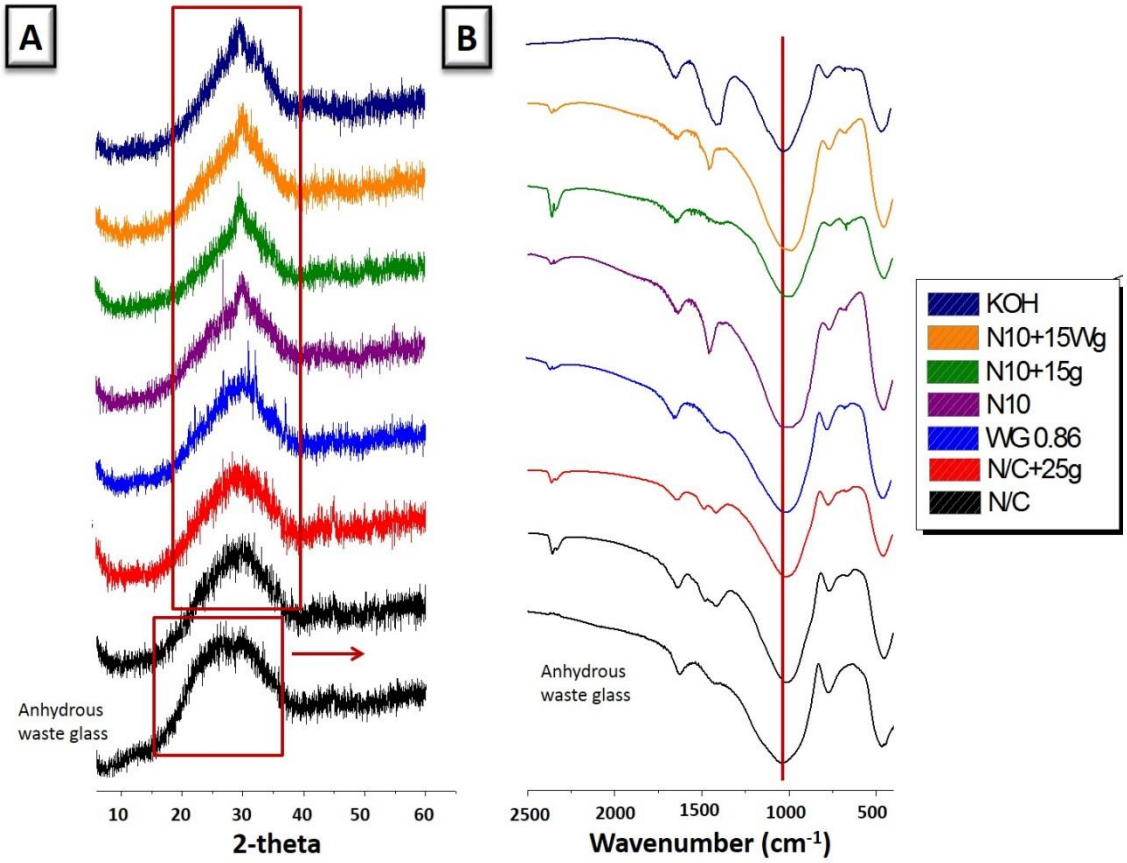

Figure 5. Unhydrated waste glass and activated waste glass pastes: **A)** XRD patterns; **B)** FTIR spectra

The FTIR spectra for the waste glass pastes prepared with the activators used in this study are shown in **Figure 5B)**. The narrow signal at 460-480 cm^{-1} was generated by the bending vibrations in the Si-O-Si bonds [57]. The likewise narrow signal at 775-800 cm^{-1} was attributed to the symmetrical stretching vibrations generated by the O-Si-O bonds [57]. An intense narrow band at around 1050 cm^{-1} was related to the asymmetrical stretching vibrations induced by bridging oxygen. Two small shoulders were observed on this signal, at 940 cm^{-1} (from non-bridging oxygen) and 1120 cm^{-1} (asymmetric vibrations from bridging oxygen in Si-O-Si bonds) [57]. The weak signal at 1460 cm^{-1} was due to the carbonate groups present in the glass [57,58].

As **Figure 5B** shows, the main band (T-O-T: Si or Al) for all the activated glass pastes was located at wavenumbers (990 to 1020 cm^{-1}) slightly lower than observed on the spectrum for the anhydrous waste glass (around 1050 cm^{-1}). That finding may be regarded as evidence of the de-polymerisation of the silica network in the waste glass [45,59]. Moreover, the former signal is normally associated with the precipitation of a silica gel that incorporates cations Ca^{2+} and Al^{3+} into its structure, for the replacement of a Si^{4+} ion with a Al^{3+} ion shifts the signal to lower frequencies. The presence of system modifiers such as Na^{+} ions also lowers the band frequency [45]. This pattern is observed irrespective of the activator used [41,60]. In this case, the shift was nonetheless less significant than observed when blast furnace slag is activated with the same alkaline solutions [33]. There, the band generated by the Si-O-Si or Al-O-Al bonds in the main reaction product is located at around 960 cm^{-1}, characteristic of the formation of a C-A-S-H gel (with a higher calcium content) [10].

Whilst carbonates were present in all the systems, the content was particularly high in the waste glass activated with KOH. The intense wide band observed at around 1424 cm^{-1} is characteristic of K_2CO_3. In that vein, paste carbonation or weathering during preparation and analysis is difficult to prevent.

- <u>SEM and BSEM/EDX</u>

The SEM micrographs of the waste glass pastes activated with the various alkaline activators and cured for 20 hours at 85 °C and 6.5 % relative humidity are shown in **Figure 6**. The waste glass pastes activated with $NaOH/Na_2CO_3$ and waterglass solutions (N/C, N/C+25g and 0.86 WG) exhibited non-uniform morphology. The unreacted (anhydrous) waste glass particles and the regions where the glass had dissolved to form the main reaction products can be clearly distinguished.

On the other hand, the morphology of the pastes activated with a high alkaline concentration (N10, N10+15g and N10+15Wg) differed, mainly due to the use of higher concentrations. These pastes contained less unreacted glass and the formation of hydration products on and from the waste glass was more visible, with a larger size that can form agglomerates of the main reaction product. No secondary zeolite-like phases were observed in these low relative humidity systems, even when the activator provided extra silica (N10+15g and N10+15Wg). Although some authors have reported that the presence of silicon sourced from the activator induces greater zeolite crystallisation [61–63], in this study, the presence of silicon in the activator was offset by the absence of aluminium, which deterred zeolite formation.

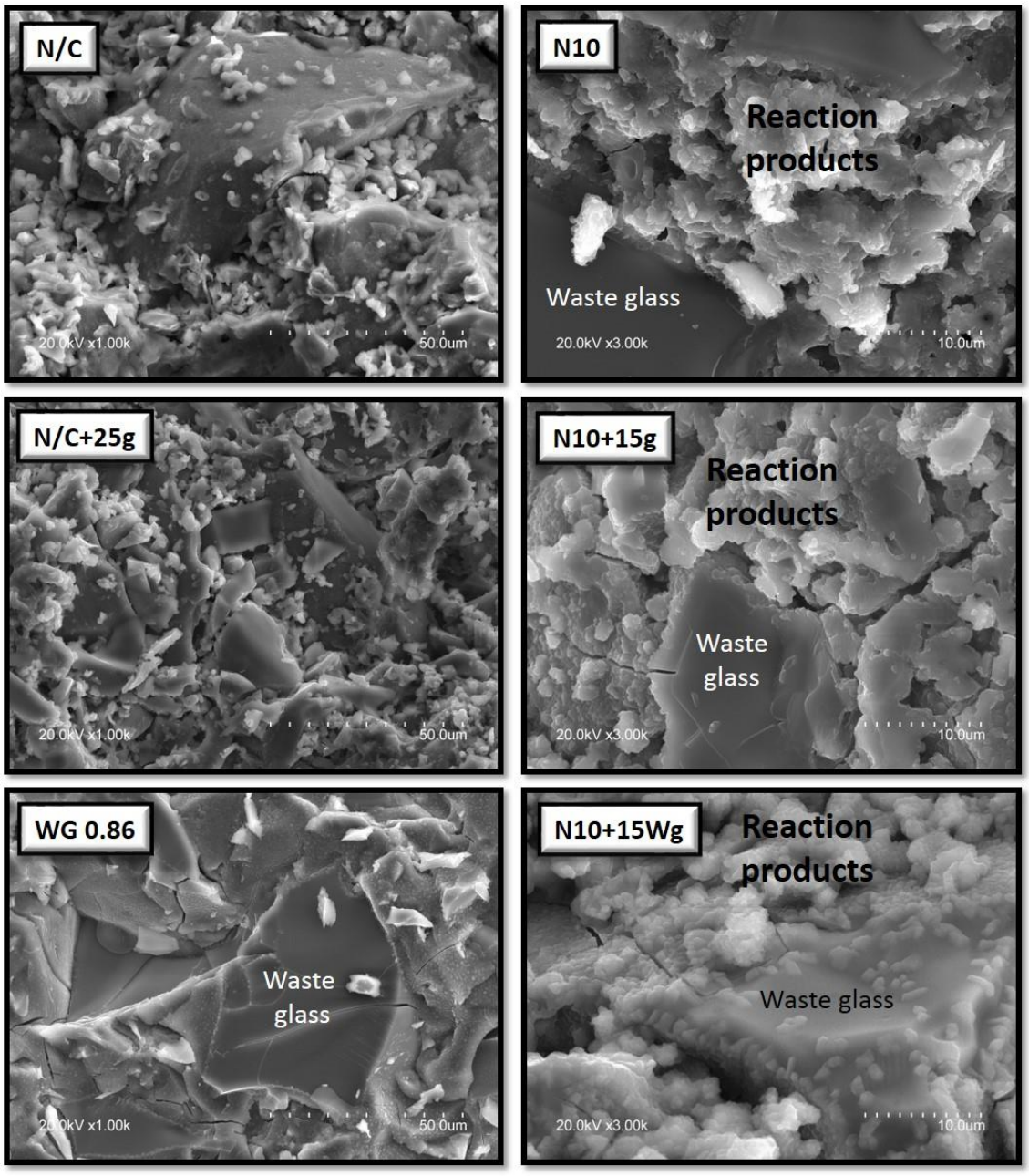

Figure 6. SEM micrograph of 1-day alkali-activated pastes cured at 85 °C and 6.5 % relative humidity

The same pattern was observed in the pastes cured at 99 % relative humidity (**Figure 7**). The microstructures of the pastes activated with NaOH-glass (N10+15g) and NaOH-Waterglass (N10+15Wg) exhibited more cracks than the materials cured at 6.5 % RH. Morphologies typical of zeolites were not identified in these pastes either, likewise as a result of the low aluminium content [64]. SEM analysis confirmed an open, scantly compact morphology, which would explain the lower strength and higher porosity of these materials.

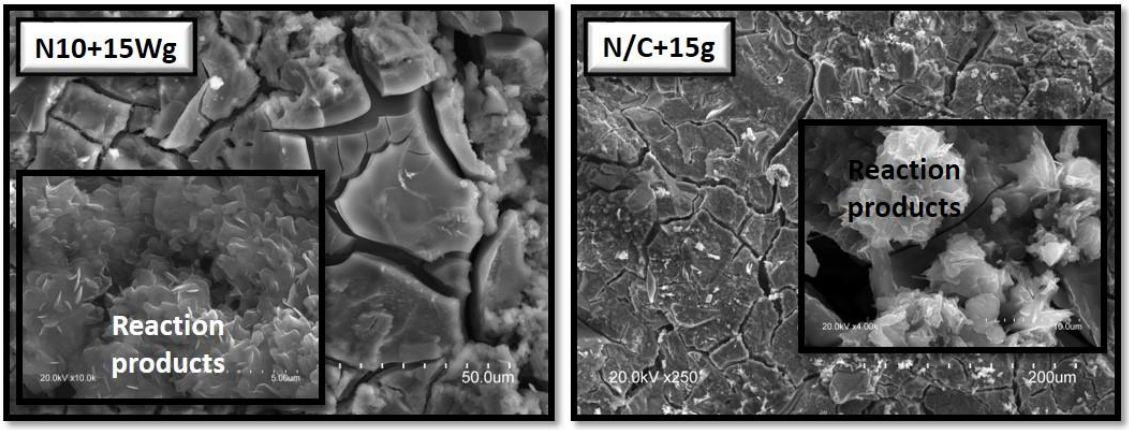

Figure 7. SEM micrograph of 1-day N10+15g and N10+15Wg pastes cured at 99 % relative humidity

The BSEM/EDX findings showed that the reaction products consisted essentially in a silicon-high Ca- and Al-low gel, irrespective of the type of activator (**Figures 8 and 9**). The Si/Al ratios in the gel formed were consequently very high (**Table 3)**.

Table 3. EDX determination of atomic ratios

Ratio	Number of analyses	Anhydrous waste glass	N/C	N/C+25g	WG 0.86	N10	N10+15g	N10+15Wg	KOH
Si/Al	20	29.81	24.12	24.74	25.01	24.52	25.31	31.26	22.77
Ca/Si	20	0.25	0.25	0.20	0.22	0.22	0.24	0.25	0.23

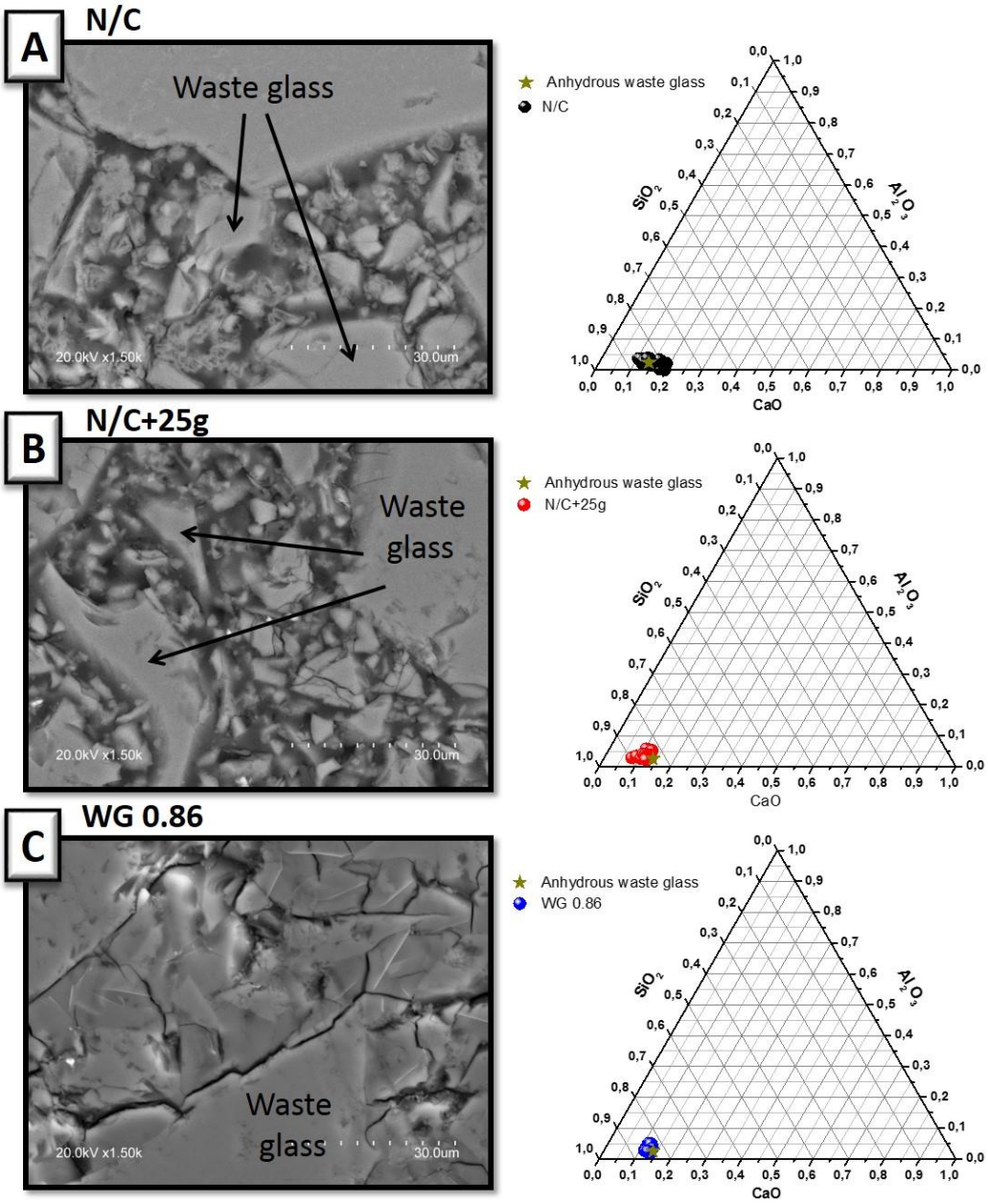

Figure 8. Chemical composition of waste glass paste hydration products after activation with: **A)** NaOH/Na_2CO_3 (N/C); **B)** NaOH/Na_2CO_3-glass (N/C+25g); **C)** waterglass (0.86 WG)

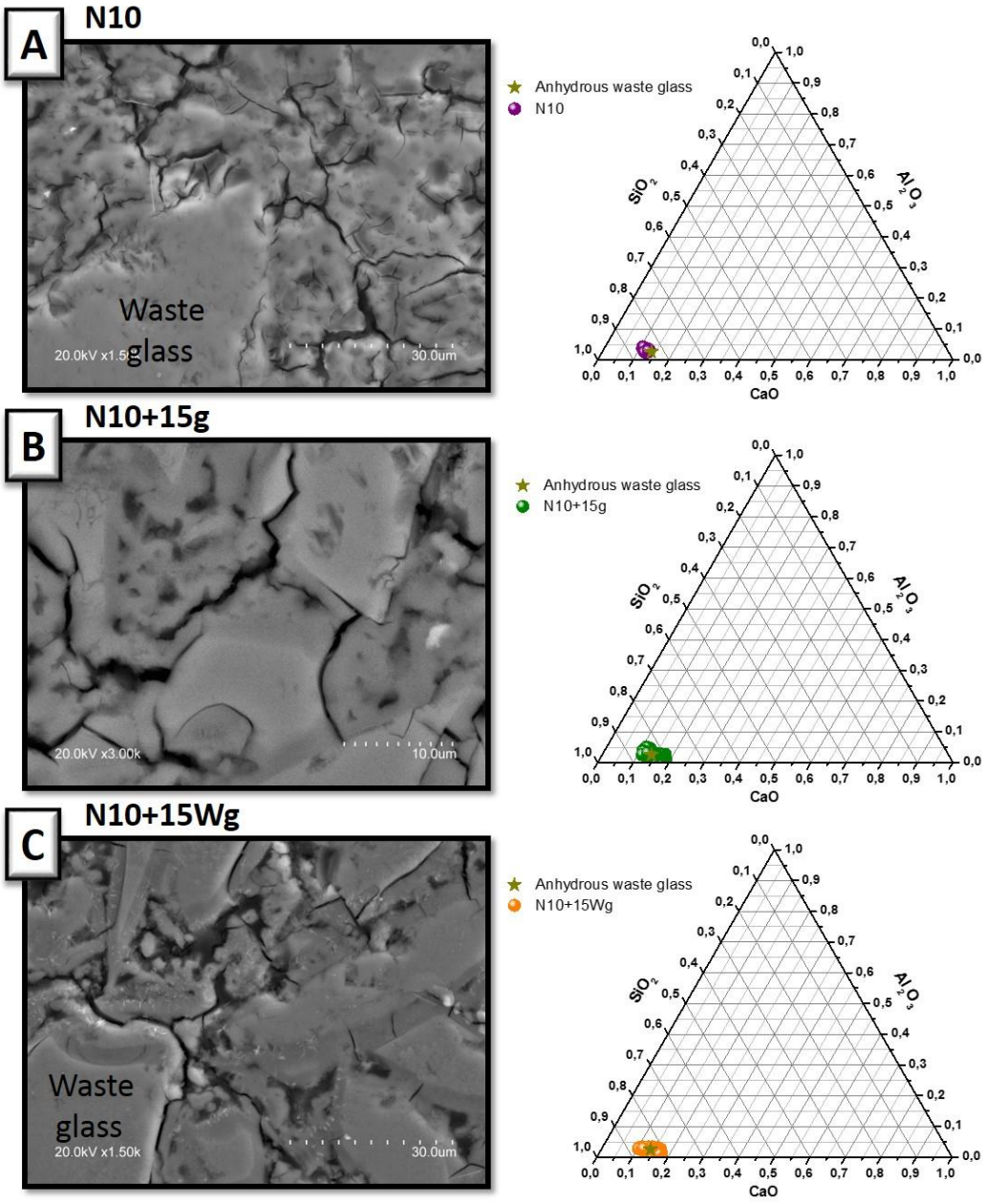

Figure 9. Chemical composition of waste glass paste hydration products after activation with: **A)** NaOH (N10); **B)** NaOH-glass (N10+15g); **C)** NaOH-waterglass (N10+15Wg)

The BSEM micrographs in **Figure 8** were obtained from the waste glass pastes activated with $NaOH/Na_2CO_3$, $NaOH/Na_2CO_3$-glass and waterglass solutions, i.e., the solutions with a concentration of 5% of Na_2O. The lighter areas in each region constitute unreacted (anhydrous) waste glass and the darker areas the reaction product, a silicon-rich gel. When the activator used was waterglass (WG 0.86), the gel formed was much more compact and uniform than the gels formed with $NaOH/Na_2CO_3$ (N/C) and $NaOH/Na_2CO_3$-glass (N/C+25g),

confirming the high mechanical strength and low porosity of the WG system. When more highly concentrated activators were used (**Figure 9**), gel morphology was more compact and less unreacted waste glass was observed. The calcium content was found in all samples, although it was still insufficient to form a C-S-H-, C-A-S-H- or (N,C)-A-S-H-like gel [10].

Lastly, the waste glass paste activated with KOH had a very compact morphology with very few microcracks. Further to the analysis in **Figure 10**, the aluminium, calcium and sodium were distributed across both the starting material and the products (gels) formed. FTIR analysis had identified potassium carbonate-like mineralogical species in these pastes.

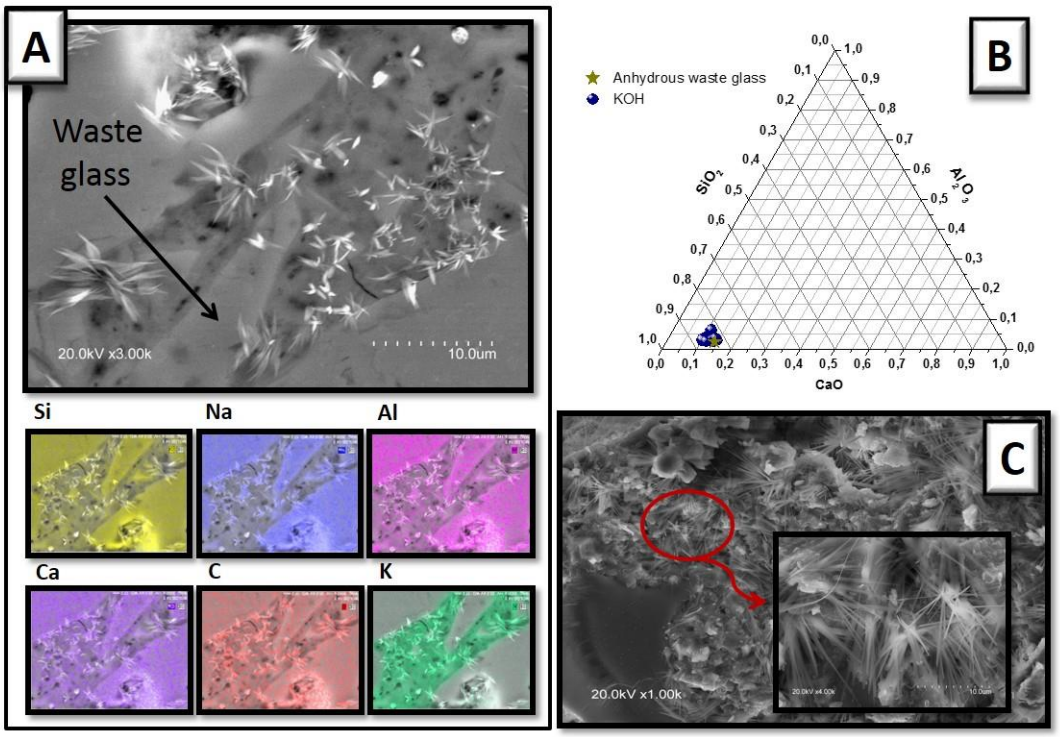

Figure 10. KOH-activated waste glass paste: **A)** BSEM map; **B)** chemical composition of hydration products; **C)** SEM micrograph

4 Discussion

This study assessed the possibility of using recycle plant waste glass as the staring material (precursor) in the preparation of alkali-activated materials (AAMs). Such application would be environmentally beneficial, for it would provide an outlet for waste glass that cannot be reused in glass manufacture.

The findings showed that the materials resulting from the alkaline activation of waste glass exhibit high mechanical strength and that curing conditions (high and low relative humidity) and the nature and concentration of the activator impacted mechanical strength and microstructure.

XRD, FTIR and SEM-BSEM--EDX exploration confirmed that the reaction product formed in the alkaline activation of waste glass is a silicon-high gel. Further to those findings, gel composition does not appear to be affected by curing conditions or activator nature or concentration. On the contrary, microstructural characteristics such as moisture-induced cracking intensity do affect gel porosity and consequently strength.

~~As both the precursors and reaction products are vitreous or amorphous materials with a low range structural order, any new phases formed are difficult to detect with XRD. Nonetheless, the position of the amorphous hump on the paste diffractograms shifted (to $2\theta = 30^\circ$-32°) due to the higher Na_2O content in the primary reaction product.~~

This main reaction product was a silicon-high gel identified by FTIR (**Figure 5B)**, in which, with the uptake into its structure of Al^{3+} and Ca^{2+}, the band observed for the paste shifted to lower wavenumbers than the signal for the unhydrated waste glass, from around 1050 cm^{-1} to 990-1020 cm^{-1}. As a rule, a high purity silica gel generates a Si-O-Si vibration band at around 1050-1100 cm^{-1}. That shift would therefore infer and be explained by some minor replacement of Si^{4+} with Al^{3+} in the main reaction product, along with the presence of a network modifier such as Na [45]. The possibility of the co-existence of this Si-high gel with other types of gels (C-S-H, C-A-S-H, N-A-S-H or (C,N)-A-S-H) was slight given the paucity of aluminium and calcium in the system and the absence of a band at around 960 cm^{-1} on the infrared spectra that would denote the presence of C-A-S-H gel [10].

Geopolymers are normally non-crystalline materials containing silicon, aluminium and sodium in the main gel. After the activation of this waste glass, however, with an aluminium-low chemical composition (**Table 1**), the gels generated are likewise Al-low (**Table 3**). Many studies have shown that the presence of aluminium in these systems, expressed as the Si/Al ratio, is directly related to mechanical strength. Although metakaolin-based geopolymers are characterised by an Si/Al ratio of around 1.8-2.0 [65,66], values of about 16 raise mechanical strength more effectively. Mechanical strength is optimal in fly ash systems when $Si/Al \approx 5$ [67], whereas in alkali-activated slag systems the optimum ranges from 2 to 4 [33,68]. As noted earlier, the low Al content explains the absence of zeolite-like secondary species in the pastes prepared in this study, where species such as sodalite hydrate ($Na_4Al_3Si_3O_{12}OH$) or Na-

chabazite ($NaAlSi_2 \cdot 3H_2O$) were lacking, for they are generally found at Si/Al ratios of 1 or 2, respectively.

The chemical composition of the AAMs produced and analysed is shown on the $CaO\text{-}Al_2O_3\text{-}SiO_2$ ternary diagrams (**Figures 8** and **9**). In the activated waste glass, the Si/Al molar ratio for the main reaction product was over 20 in all systems due to the low aluminium content in the starting material (around 2.05 %) (**Table 3**). The calcium content (Ca/Si ranging from 0.20 to 0.25), in turn, was lower than in the materials obtained in blast furnace slag activation. Several authors have shown the latter to have a Ca/Si molar ratio of 0.8-1.2, depending on the activator [33,68]. Due more than likely to the chemical composition of the waste glass used as a precursor (Si-high and Al- and Ca-low), the alkali-activated products were scantly affected by the activating conditions.

The microstructure developing in the pastes did appear to be impacted by the activating conditions (**Figure 7**). Low (6.5 %) humidity thermal curing yielded a much more cohesive microstructure with fewer macropores and microcracks and higher mechanical strength than high (99 %) relative humidity curing. The BET findings appeared to indicate that the gel forming at low RH had greater microporosity and specific surface than the gel in the high RH pastes. Both these favourable characteristics would also help explain the higher mechanical performance in the former.

The findings illustrated in **Figure 2** infer that the curing conditions (relative humidity) had a likewise significant impact on strength development in the waste glass pastes activated by all the solutions used except KOH. Whilst a number of studies have analysed changes in alkali-activated materials properties under different curing temperatures [7,69–72], very few have been conducted on the effect of relative humidity on curing [73,74]. One possible explanation for the higher mechanical strength when the pastes were heat-cured at a lower relative humidity is the significant role played by the water (adsorbed, absorbed or both) present in the this materials and its subsequent evaporation in the generation of a product with fewer microcracks or micropores [73]. During the dissolution of (very aluminium-low) waste glass in a highly alkaline medium, the water available in the aqueous phase to form $Si(OH)_4$ and $Al(OH)_4$ monomers is partially released during subsequent polymerisation [73]. The reaction between the glass and the OH^- groups always hydrolyses oxygen bridges, partially destroying the network [35,75]. In alkaline media, glass may be said to be depolymerised, resulting in total destruction of its network and gradual dissolution [35,75]. Low RH leads to the formation of more cohesive AAMs with a smaller pore size, as the Hg porosimetry and BET findings showed (**Figures 3** and **4**). The N10+15g sample exhibited the lowest total porosity and a higher specific

surface with fewer <1 nm pores in the gel. Silicon-high gels tend to have a high specific surface and adsorb much of the water in the medium [45]. In dryer environments, much more compact systems are formed, as water is eliminated from the pores, inducing the formation of a less porous, more cohesive gel.

In connection with activator nature and concentration, the solutions that induced the formation of pastes with higher mechanical strength were the ones with a high OH^- ion content. The OH^- ions favoured the breakage of the Si-O-Si bonds in the glass, prompting more intense dissolution and generating reaction products that afforded the system suitable mechanical stability [75]. Moreover, the silicon-containing solutions (0.86 WG) delivered higher strength materials than the $NaOH/Na_2CO_3$ solution because silicon favoured glass activation.

When the KOH solution was used as the waste glass activator, strength varied very little between the specimens cured at high and low relative humidity. From the compositional standpoint, however, all the systems generated the same main reaction product (silicon-high gel), irrespective of the nature and concentration of the activator (**Figures 8, 9** and **10**). The cation effect on precursor dissolution was likewise significant. Cation K^+ dissolves less of the Ca and Mg present in glass and, having a lower charge density than cation Na^+, induces a smaller proportion of secondary products [54]. This study revealed differences between sodium- and potassium-based activators in terms of strength development and microstructure [44]. One of the determining factors in reaction kinetics is cation size. As Na^+ is smaller, it forms zeolites more readily [54].

The solution pH, however, was observed to affect the formation of the reaction product, with higher values generating a more cohesive, higher strength gel. The use of solutions with a high alkaline content (N10, N10+15g and N10+15Wg) delivered a much more compact microstructure (more compact hydration products) (**Figure 6**), as confirmed by the significant decline in total porosity in the systems with highest mechanical performance. Moreover, the more alkaline solutions dissolved the waste glass more effectively, raising system reactivity and favouring the formation of more primary reaction product.

The BET study of these systems revealed a correlation between the specific surface of the systems and the RH at which they were cured. At low (6.5 %) RH, paste specific surface was higher. That in turn induced lower total porosity and enhanced pore size refinement, raising 1-day mechanical strength.

The results obtained after the activation of waste glass with different alkaline activators and under different curing conditions provided us information at short study ages (1 day) in pastes, thus leaving a door open in the investigation of these AAMs at more advanced ages and in materials intended for an application in construction, such as in concrete. Moreover, a need has been identified for future studies geared to determining the chemical and physical stability of pastes generated by the alkaline activation of waste glass in aggressive media, for Si-high gels are known to exhibit dimensional or chemical instability or both.

5 Conclusions

The main conclusions drawn from the present findings are listed below.

- Waste glass is apt as a precursor for alkaline cements, for it develops materials with suitable mechanical strength.
- The main reaction product obtained in waste glass activation is an alkali-activated material (AAM). The composition of this silicon-high, Al- and Ca-low gel is unaffected by activation conditions or the nature or concentration of the alkaline activator.
- Curing conditions, and more specifically relative humidity, have a significant effect on strength development in alkali-activated glass pastes. When cured for 20 hours at 85±2 °C and 6.5 % relative humidity, the pastes developed strength 50-75 % greater than when cured for the same time and at the same temperature but at 99 % relative humidity.
- High alkaline activator concentrations induce the formation of less porous, higher strength pastes with more compact microstructures.
- The absence of zeolite-like secondary reaction products would be explained by the low Al content in the precursor waste glass.

6 Acknowledgements

This research was funded by the Ministry of Economy and Competitiveness under projects BIA2010-15516 and BIA2013-47876-C2-1-P and the Spanish National Research Council under project PIE201460E06. The authors wish to thank Eduardo Torroja Institute for Construction Science technicians Alfredo Gil, Francisco Morales and Patricia Rivilla for their assistance with the laboratory trials.

7 References

[1] A.O. Purdon, The action of alkalis on blast-furnace slag, J. Soc. Chem. Ind.-Trans. Commun. 59 (1940) 191–202.

[2] V. Glukhovsky, G. Rostovskaja, G. Rumyna, High strength slag-alkaline cements, in: 7th Int. Congr. Chem. Cem, Paris, 1980: pp. 164–168.

[3] V. Glukhovsky, Y. Zaitsev, V. Pakhomow, Slag-alkaline cements and concretes structures, properties, technological and economic aspects of the use, Silic. Ind. 48 (1983) 197–200.

[4] J. Davidovits, Geopolymer Chemistry and Applications, Institud Géopolymère, San Quintin, France, 2008.

[5] S.A. Bernal, E.D. Rodríguez, R. Mejia de Gutiérrez, J.L. Provis, S. Delvasto, Activation of Metakaolin/Slag Blends Using Alkaline Solutions Based on Chemically Modified Silica Fume and Rice Husk Ash, Waste and Biomass Valorization. 3 (2011) 99–108.

[6] A. Palomo, M.T. Blanco-Varela, M.L. Granizo, F. Puertas, T. Vazquez, M.W. Grutzeck, Chemical stability of cementitious materials based on metakaolin, Cem. Concr. Res. 29 (1999) 997–1004.

[7] S. Alonso, A. Palomo, Alkaline activation of metakaolin and calcium hydroxide mixtures: influence of temperature, activator concentration and solids ratio, Mater. Lett. 47 (2001) 55–62.

[8] E. Robayo, R.M. de Gutierrez, M. Gordillo, Natural pozzolan-and granulated blast furnace slag-based binary geopolymers, Mater. Constr. 66 (2016) e077.

[9] F. Puertas, Cementos de escorias activadas alcalinamente: Situación actual y perspectivas de futuro, Mater. Construcción. 45 (1995) 53–64.

[10] F. Puertas, M. Palacios, H. Manzano, J.S. Dolado, A. Rico, J. Rodríguez, A model for the C-A-S-H gel formed in alkali-activated slag cements, J. Eur. Ceram. Soc. 31 (2011) 2043–2056.

[11] F. Puertas, Escorias de alto horno: composición y comportamiento hidráulico, Mater. Construcción. 43 (1993).

[12] S.A. Bernal, R. San Nicolas, R.J. Myers, R. Mejía de Gutiérrez, F. Puertas, J.S.J. van Deventer, J.L. Provis, MgO content of slag controls phase evolution and structural changes induced by accelerated carbonation in alkali-activated binders, Cem. Concr. Res. 57 (2014) 33–43.

[13] C. Shi, P. Krivenko, D. Roy, Alkali-Activated Cements and Concretes, Taylor and Francis, London and New York, 2006.

[14] A. Palomo, P. Krivenko, E. Kavalerova, O. Maltseva, A review on alkaline activation: new analytical perspectives, Mater. Construcción. 64 (2014).

[15] A. Cornejo, C. Leiva, L.F. Vilches, Properties of fly ash and metakaolín based geopolymer panels under fire resistance tests, Mater. Construcción. 65 (2015) e059.

[16] C. Shi, A. Fernández-Jiménez, Stabilization/solidification of hazardous and radioactive wastes with alkali-activated cements., J. Hazard. Mater. 137 (2006) 1656–63.

[17] I. Escalante-García, Overview of the potential of urban waste glass as a cementitious material in alternative chemically activated binders, in: 14th Int. Congr. Chem. Cem., Beijing, 2015: p. 25.

[18] Ecovidrio, Ecovidrio, Http://www.ecovidrio.es/. (2015).

[19] R.G. Pike, D. Hubbard, E.S. Newman, Binary silicate glasses in the study of alkali-aggregate reaction, High Res Board Bull. 275 (1960) 39–44.

[20] A. Scmidt, W.H.F. Saia, Alkali-aggregate reaction tests on glass used for exposed aggregate wall panel work, ACI Mater. J. 60 (1963) 1235–1236.

[21] C.D. Johnston, Waste glass as coarse aggregate for concrete, J. Test Eval. 2 (1974) 344–350.

[22] C. Meyer, S. Baxter, W. Jin, Alkali-aggregate reaction in concrete with waste glass as aggregate, in: Proc. 4th Mater. Eng. Conf. Mater. New Millenn., Reston, 1996: pp. 1388–1397.

[23] C. Meyer, S. Baxter, Use of recycled glass and fly ash for precast concrete, J. Mater. Civ. Eng. Civ. Eng. 11 (1999) 89–90.

[24] C. Pollery, S.M. Cramer, R.V. De la Cruz, Potential for using waste glass in portland cement concrete, J. Mater. Civ. Eng. Civ. Eng. 10 (1998) 210–219.

[25] Z.P. Bazant, G. Zi, C. Meyer, Fracture mechanics of ASR in concretes with waste glass particles of different sizes, J. Eng. Mech. 126 (2000) 226–232.

[26] E.A. Byars, B. Morales-Hernandez, H.Y. Zhu, Waste glass as concrete aggregate and pozzolan, Concrete. 38 (2004) 41–44.

[27] I.B. Topcu, M. Canbaz, Properties of concrete containing waste glass, Cem. Concr. Compos. 34 (2004) 267–274.

[28] C.H. Chen, R. Huang, J.K. Wu, C.C. Yang, Waste E-glass Particles used in cementitious mixtures, Cem. Concr. Res. 36 (2006) 449–456.

[29] G. Chen, H. Lee, K.L. Young, P.L. Yue, A. Wong, T. Tao, K.K. Choi, Glass recycling in cement production--an innovative approach., Waste Manag. 22 (2002) 747–753.

[30] C. Shi, K. Zheng, A review on the use of waste glasses in the production of cement and concrete, Resour. Conserv. Recycl. 52 (2007) 234–247.

[31] Z. Xie, Y. Xi, Use of recycled glass as a raw material in the manufacture of Portland cement, Mater. Struct. 35 (2002) 510–515.

[32] A. Khmiri, M. Chaabouni, B. Samet, Chemical behaviour of ground waste glass when used as partial cement replacement in mortars, Constr. Build. Mater. 44 (2013) 74–80.

[33] F. Puertas, M. Torres-Carrasco, Use of glass waste as an activator in the preparation of alkali-activated slag. Mechanical strength and paste characterisation, Cem. Concr. Res. 57 (2014) 95–104.

[34] M. Torres-Carrasco, F. Puertas, Waste glass in the geopolymer preparation. Mechanical and microstructural characterisation, J. Clean. Prod. 90 (2015) 397–408.

[35] M. Torres-Carrasco, J.G. Palomo, F. Puertas, Sodium silicate solutions from dissolution of glass wastes: Statistical analysis, Mater. Construcción. 64 (2014).

[36] M. Torres-Carrasco, M. Tognonvi, A. Tagnit-Hamou, F. Puertas, Durability of Alkali-Activated Slag Concretes Prepared using waste glass as Alternative activator, ACI. 112 (2015) 791–800.

[37] F. Puertas, M. Torres-Carrasco, M.M. Alonso, Reuse of urban and industrial waste glass as novel activator for alkali-activated slag cement pastes: a case study, in: Handb. Alkali-Activated Cem. Mortars Concr., 2014: pp. 75–110.

[38] H.K. Tchakouté, C.H. Rüscher, S. Kong, E. Kamseu, C. Leonelli, Geopolymer binders from metakaolin using sodium waterglass from waste glass and rice husk ash as alternative activators: A comparative study, Constr. Build. Mater. 114 (2016) 276–289.

[39] L.K. Turner, F.G. Collins, Carbon dioxide equivalent (CO_2) emissions: A comparison between geopolymer and OPC cement concrete, Constr. Build. Mater. 43 (2013) 125–130.

[40] I. Garcia-Lodeiro, E. Aparicio-Rebollo, A. Fernández-Jimenez, A. Palomo, Effect of calcium on the alkaline activation of aluminosilicate glass, Ceram. Int. 42 (2016) 7697–7707.

[41] I. Garcia-Lodeiro, A. Fernández-Jimenez, P. Pena, A. Palomo, Alkaline activation of synthetic aluminosilicate glass, Ceram. Int. 40 (2014) 5547–5558.

[42] B. Walkley, R. San Nicolas, M.-A. Sani, G.J. Rees, J. V. Hanna, J.S.J. van Deventer, J.L. Provis, Phase evolution of C-(N)-A-S-H/N-A-S-H gel blends investigated via alkali-activation of synthetic calcium aluminosilicate precursors, Cem. Concr. Res. 89 (2016) 120–135.

[43] B. Walkley, R. San Nicolas, M.-A. Sani, J.D. Gehman, J.S.J. van Deventer, J.L. Provis, Phase evolution of Na_2O–Al_2O_3 –SiO_2 –H_2O gels in synthetic aluminosilicate binders, Dalt. Trans. 45 (2016) 5521–5535.

[44] M. Cyr, R. Idir, T. Poinot, Properties of inorganic polymer (geopolymer) mortars made of glass cullet, J. Mater. Sci. 47 (2011) 2782–2797.

[45] R. Redden, N. Neithalath, Microstructure , strength , and moisture stability of alkali activated glass powder-based binders, Cem. Concr. Compos. 45 (2014) 46–56.

[46] U. Avila-López, J.M. Almanza-Robles, J.I. Escalante-García, Investigation of novel waste glass and limestone binders using statistical methods, Constr. Build. Mater. 82 (2015) 296–303.

[47] R. Martinez-Lopez, J. Ivan Escalante-Garcia, Alkali activated composite binders of waste silica soda lime glass and blast furnace slag: Strength as a function of the composition, Constr. Build. Mater. 119 (2016) 119–129.

[48] G. Kovalchuk, A. Jiménez-Fernández, A. Palomo, Alkali-activated fly ash: effect of termal curing conditions on mechanical and microstructural development-Part II, Fuel. 86 (2007) 315–322.

[49] P.V. Krivenko, G. Kovalchuk, Fly ash based zeolite cements. Innovations and developments in concrete materials and construction, in: Challenges Concr. Constr., Dundee, 2002: pp. 123–132.

[50] P.V. Krivenko, G. Kovalchuk, G. Yu, Heat-resistant fly ash based geocements, in: Geopolymer 2002, Melbourne, Australia, 2002.

[51] G. Kovalchuk, G. Yu, Heat resistant gas concrete based on alkaline aluminosilicate binder, Ukrainian, 2002.

[52] M. Criado, A. Palomo, A. Fernández-Jiménez, Alkali activation of fly ashes. Part 1: Effect of curing conditions on the carbonation of the reaction products, Fuel. 84 (2005) 2048–2054.

[53] K. Yang, J. Song, Workability Loss and Compressive Strength Development of Cementless Mortars Activated by Combination of Sodium Silicate and Sodium Hydroxide, J. Mater. Civ. Eng. Civ. Eng. 21 (2009) 119–127.

[54] A. Fernández-Jiménez, A. Palomo, M. Criado, Alkali activated fly ash binders. A comparative study between sodium and potassium activators, Mater. Construcción. 56 (2006) 51–65.

[55] H. Xu, J.S.J. Van Deventer, The effect of alkali metals on the formation of geopolymeric gels from alkali-feldspars, Colloids Surfaces A Physicochem. Eng. Asp. 216 (2003) 27–44.

[56] R.T. Hemmings, E.E. Berry, On the Glass in Coal Fly Ashes: Recent Advances, Mater. Res. Soc. 113 (1987).

[57] S.M. Abo-Naf, F.H. El Batal, M.A. Azooz, Characterization of some glasses in the system SiO_2, Na_2O·RO by infrared spectroscopy, Mater. Chem. Phys. 77 (2002) 846–852.

[58] M.A. Villegas, J.M. Fernández-Navarro, Preparación y caracterización de vidrios del sistema CaO-SiO_2 por el procedimiento sol-gel, Bol. La Soc. Cerámica Y Vidr. 27 (1988) 349–357.

[59] I. García-Lodeiro, A. Fernández-Jiménez, M.T. Blanco, A. Palomo, FTIR study of the sol-gel synthesis of cementitious gels: C-S-H and N-A-S-H, J. Sol-Gel Sci. Technol. 45 (2008) 63–72.

[60] C.I. Merzbacher, W.B. White, The structure of alkaline earth aluminosilicate glasses as determined by vibrational spectroscopy, J. Non. Cryst. Solids. 130 (1991) 18–34.

[61] M. Criado, A. Fernández-Jiménez, A. Palomo, Alkali activation of fly ash: Effect of the SiO_2/Na_2O ratio, Microporous Mesoporous Mater. 106 (2007) 180–191.

[62] M. Criado, A. Fernández-Jiménez, A. Palomo, I. Sobrados, J. Sanz, Effect of the SiO_2/Na_2O ratio on the alkali activation of fly ash. Part II: ^{29}Si MAS-NMR Survey, Microporous Mesoporous Mater. 109 (2008) 525–534.

[63] J.L. Provis, G.C. Luckey, J.S.J. Van Deventer, Do Geopolymers actually contain nanocrystalline zeolites? A reexamination of existing results, Chem. Mater. 17 (2005) 3075–3085.

[64] D.W. Breck, Zeolite molecular sieves: Structure, chemistry and Uses, New York, USA, 1973.

[65] P. Duxson, J.L. Provis, G.C. Luckey, S.W. Mallicoat, W.M. Kriven, J.S.J. Van Deventer, Understanding the relationship between geopolymer composition, microstructure and mechanical properties, Colloids Surfaces A Physicochem. Eng. Asp. 269 (2005) 47–58.

[66] P. Duxson, S.W. Mallicoat, G.C. Lukey, W.M. Kriven, J.S.J. van Deventer, The effect of alkali and Si/Al ratio on the development of mechanical properties of metakaolin based geopolymers, Colloids Surfaces A Physicochem. Eng. Asp. 292 (2007) 8–20.

[67] A. Palomo, M.W. Grutzeck, M.T. Blanco, Alkali-activated fly ashes A cement for the future, Cem. Concr. Res. 29 (1999) 1323–1329.

[68] F. Puertas, A. Fernández-Jiménez, M.. Blanco-Varela, Pore solution in alkali-activated slag cement pastes. Relation to the composition and structure of calcium silicate hydrate, Cem. Concr. Res. 34 (2004) 139–148.

[69] E. Altan, S.T. Erdoğan, Alkali activation of a slag at ambient and elevated temperatures, Cem. Concr. Compos. 34 (2012) 131–139.

[70] G.F. Huseien, J. Mirza, M. Ismail, M.W. Hussin, Influence of different curing temperatures and alkali activators on properties of GBFS geopolymer mortars containing fly ash and palm-oil fuel ash, Constr. Build. Mater. 125 (2016) 1229–1240.

[71] P. Nath, P.K. Sarker, Fracture properties of GGBFS-blended fly ash geopolymer concrete cured in ambient temperature, Mater. Struct. 50 (2017) 32–44.

[72] A.A. Aliabdo, A.E.M. Abd Elmoaty, H.A. Salem, Effect of cement addition, solution resting time and curing characteristics on fly ash based geopolymer concrete performance, Constr. Build. Mater. 123 (2016) 581–593.

[73] D.S. Perera, O. Uchida, E.R. Vance, K.S. Finnie, Influence of curing schedule on the integrity of geopolymers, J. Mater. Sci. 42 (2007) 3099–3106.

[74] A. Tawfik, F.A. El-raoof, H. Katsuki, K.J.D. Mackenzie, S. Komarneni, K-Based Geopolymer from metakaolin: roles of K / Al ratio and water or steam Curing at different temperatures, Mater. Constr. 66 (2016) e081.

[75] J.M. Fernández-Navarro, El vidrio, Editorial CSIC, Madrid, 2003.